

# Bell states and entanglement of two-dimensional polar molecules in electric fields

Ying-Yen Liao\*

*Department of Applied Physics, National University of Kaohsiung, Kaohsiung 811, Taiwan*

(Dated: December 1, 2016)

Entanglement generated from polar molecules of two-dimensional rotation is investigated in a static electric field. The electric field modulates the rotational properties of molecules, leading to distinctive entanglement. The concurrence is used to estimate the degree of entanglement. When the electric field is applied parallel or perpendicular to the intermolecular direction, the concurrences reveal two overlapping features. Such a pronounced signature corresponds to the coexistence of all Bell-like states. The characteristics of Bell-like states and overlapping concurrences are kept independent of the modulation of dipole-field and dipole-dipole interactions. On the contrary, the Bell-like states fail to coexist in other field directions, reflecting nonoverlapping concurrences. Furthermore, the thermal effect on the entanglement is analyzed for the Bell-like states. Dissimilar suppressed concurrences occur due to different energy structures for the two specific field directions.

PACS numbers: 03.67.Mn, 03.65.Ud, 33.20.Sn

## I. INTRODUCTION

Exploring entanglement has attracted considerable interest in various physical systems, ranging from atoms and photons to solid-state materials [1–4]. Entanglement describes a phenomenon in which two or more subsystems are linked through direct or indirect interactions. This a quantum phenomenon has become an essential ingredient in quantum information processing [5, 6]. Among various architectures, a bipartite system is a fundamental unit to exploit the nature of entanglement. Fascinating properties have been extracted from a variety of bipartite systems. The Bell state is a representative example, which plays an important role in dense coding protocol [7], quantum teleportation [8], and entanglement swapping [9]. As a result, generating entanglement becomes an indispensable step for follow-up operations and further applications.

Two polar molecules can form a platform for generating entanglement directly through dipole-dipole interaction. This molecular platform provides an advantage of controllable rotational properties via the coupling of external fields with the dipole moment [10–12]. Field sources include static electric fields [13, 14], laser pulses [15], and optimized complex pulses [16]. The rotational properties, such as energy and wave function, are modified to affect the entanglement as well as the dipole-dipole interaction. In most studies, polar molecules are considered to rotate in three dimensions. However, only minor efforts have been made that focus on the entanglement generated by two-dimensional rotation. The energies, level degeneracy, and wave functions of a two-dimensional rotor are different from those of a three-dimensional rotor [17]. Two-dimensional rotational manner has been observed in the experiments of hydrogen on a surface [18–20]. The planar rotation in diverse configurations

further leads to interesting consequences for energy spectrum [21, 22], molecular orientation [23], and specific heat [24, 25]. In this work we study the entanglement in a system of two polar molecules confined to a plane. Both molecules rotate in two dimensions, which are modified by applying an in-plane electric field. We use concurrence to qualify the degree of entanglement by orienting the electric field. For specific field directions, all Bell-like states are jointly displayed, corresponding to a situation of overlapping concurrences. Specifically, Bell-like states are robustly maintained when the dipole-field and dipole-dipole interactions are tuned. On the contrary, these pronounced properties are destroyed in an electric field of another direction. The obtained results are different from those in the three-dimensional cases. We further analyze the thermal effect on the entanglement for the Bell-like states.

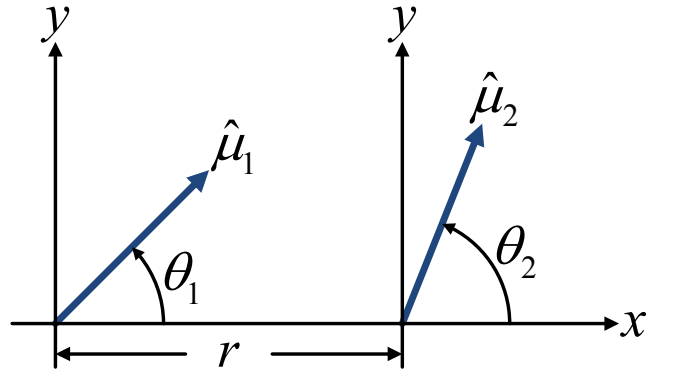


FIG. 1. Schematic diagram of two polar molecules separated by a distance  $r$ . The left and right molecules are confined to two-dimensional motion, corresponding to the unit vectors of the dipole moments  $\hat{\mu}_1 = (\cos \theta_1, \sin \theta_1)$  and  $\hat{\mu}_2 = (\cos \theta_2, \sin \theta_2)$ , respectively.

\* yyiao@nuk.edu.tw

## II. MODEL AND THEORY

We consider two polar diatomic molecules of rotational constant  $B$  and dipole moment  $\mu$  confined to a plane as depicted in Fig. 1. Both molecules rotate in two dimensions, which are spatially separated by an interval  $r$ . A static electric field of strength  $\varepsilon$  and tilt angle  $\theta_t$  is applied to couple with the dipole moments of the molecules. The modified two-dimensional rotation leads to specific dipole-dipole interaction. The Hamiltonian describing the system is

$$H = \sum_{i=1}^2 H_0^i + V_d, \quad (1)$$

with

$$H_0^i = -B \frac{d^2}{d\theta_i^2} - \omega (\cos \theta_t \cos \theta_i + \sin \theta_t \sin \theta_i), \quad (2)$$

$$V_d = \Omega [\hat{\mu}_1 \cdot \hat{\mu}_2 - 3 (\hat{\mu}_1 \cdot \hat{u}_x) (\hat{\mu}_2 \cdot \hat{u}_x)], \quad (3)$$

where  $\omega = \mu\varepsilon$  is the strength of dipole-field interaction,  $\Omega = \mu^2/4\pi\epsilon_0 r^3$  is the strength of dipole-dipole interaction,  $\hat{\mu}_i = (\cos \theta_i, \sin \theta_i)$  is the unit vector of the dipole moment,  $\hat{u}_x = (1, 0)$  is the unit vector,  $\epsilon_0$  is the permittivity of free space, and  $\theta_i$  is the polar angle between the molecular axis and the  $x$  axis for the left ( $i = 1$ ) and right ( $i = 2$ ) molecules. From the coordinates of the molecules, the dipole-dipole interaction  $V_d$  is given by

$$V_d = \Omega (\sin \theta_1 \sin \theta_2 - 2 \cos \theta_1 \cos \theta_2). \quad (4)$$

The magnitudes of  $\omega$  and  $\Omega$  in Eqs. (2) and (4) are dependent on the dipole moment, field strength, and intermolecular distance.

For a single molecule in an electric field, the field-dependent energy  $\varepsilon_l$  and its corresponding wave function  $\psi_l$  are obtained from the equation

$$H_0 \psi_l = \varepsilon_l \psi_l, \quad (5)$$

where the index  $i$  is omitted and the positive integer  $l$  is defined from 0. The wave function  $\psi_l$  is described by

$$\psi_l(\theta) = \sum_m c_m^l \varphi_m(\theta), \quad (6)$$

where  $c_m^l$  is the expanded coefficient,  $\varphi_m(\theta) = \exp(im\theta)/\sqrt{2\pi}$  is the field-free eigenfunction, corresponding to the energy  $m^2 B$  for  $m = 0, \pm 1, \pm 2, \dots$  [17].

The effect of the dipole-dipole interaction on the system is captured by employing the lowest two states of the molecules. The chosen states are the ground state  $|0_i\rangle = |\psi_0^i(\theta_i)\rangle$  and the first excited state  $|1_i\rangle = |\psi_1^i(\theta_i)\rangle$ , corresponding to the energies  $\varepsilon_0$  and  $\varepsilon_1$ , respectively.

Here the index  $i$  is restored. To solve the Hamiltonian in Eq. (1), a composite state is taken by the form

$$|\Psi_n\rangle = d_1^n |00\rangle + d_2^n |01\rangle + d_3^n |10\rangle + d_4^n |11\rangle, \quad (7)$$

where  $d_j^n$  is the coefficient, and  $|00\rangle = |0_1\rangle \otimes |0_2\rangle$ ,  $|01\rangle = |0_1\rangle \otimes |1_2\rangle$ ,  $|10\rangle = |1_1\rangle \otimes |0_2\rangle$ , and  $|11\rangle = |1_1\rangle \otimes |1_2\rangle$  are the basis states. By using  $|\Psi_n\rangle$ , the energy  $E_n$  and the coefficient  $d_j^n$  can be derived from the matrix

$$\tilde{H} = \begin{pmatrix} \delta_{0,0} + \Gamma_{0,0} & \Gamma_{0,X} & \Gamma_{0,X} & \Gamma_{X,X} \\ \Gamma_{0,X}^* & \delta_{0,1} + \Gamma_{0,1} & \Gamma_{X,XC} & \Gamma_{1,X} \\ \Gamma_{0,X}^* & \Gamma_{X,XC} & \delta_{0,1} + \Gamma_{0,1} & \Gamma_{1,X} \\ \Gamma_{X,X}^* & \Gamma_{1,X}^* & \Gamma_{1,X}^* & \delta_{1,1} + \Gamma_{1,1} \end{pmatrix}, \quad (8)$$

with  $\delta_{\alpha,\beta} = \varepsilon_\alpha + \varepsilon_\beta$  and  $\Gamma_{\alpha,\beta} = \Omega(S_\alpha S_\beta - 2C_\alpha C_\beta)$  for  $\alpha$  and  $\beta$  being 0, 1,  $X$ , and  $XC$ . The factors are expressed as  $C_{0(1)} = \langle \psi_{0(1)}^i | \cos \theta_i | \psi_{0(1)}^i \rangle$ ,  $S_{0(1)} = \langle \psi_{0(1)}^i | \sin \theta_i | \psi_{0(1)}^i \rangle$ ,  $C_{X(XC)} = \langle \psi_{0(1)}^i | \cos \theta_i | \psi_{1(0)}^i \rangle$ , and  $S_{X(XC)} = \langle \psi_{0(1)}^i | \sin \theta_i | \psi_{1(0)}^i \rangle$ .

The density matrix method is used to examine the entanglement properties in the system [26–28]. Based on  $E_n$  and  $|\Psi_n\rangle$ , the density matrix can be described as

$$\rho = \frac{\sum_{n=1}^4 \exp(-E_n/k_B T) |\Psi_n\rangle \langle \Psi_n|}{\sum_{n=1}^4 \exp(-E_n/k_B T)}, \quad (9)$$

with the Boltzmann constant  $k_B$  and temperature  $T$ . The degree of entanglement can be measured by the concurrence

$$C = \max \left\{ 0, \sqrt{\lambda_1} - \sqrt{\lambda_2} - \sqrt{\lambda_3} - \sqrt{\lambda_4} \right\}, \quad (10)$$

where the quantities  $\lambda_k$  are the eigenvalues of the matrix

$$\tilde{\rho} = \rho (\sigma_y \otimes \sigma_y) \rho^* (\sigma_y \otimes \sigma_y), \quad (11)$$

in decreasing order. The operator  $\sigma_y$  is the Pauli matrix and  $\rho^*$  is the complex conjugate of  $\rho$ . The value of the concurrence ranges from zero to one, corresponding to an unentangled state and a maximally entangled state, respectively.

## III. NUMERICAL RESULTS AND DISCUSSION

In this work the systemic properties are explored by controlling the strength of the dipole-field interaction  $\omega$  and the dipole-dipole interaction  $\Omega$ . The energy-related quantities are expressed in units of  $B$  throughout the calculations. Figure 2(a) shows the energy spectra of a single molecule in an electric field of  $\theta_t = 0^\circ$ , i.e., the field direction lies along the  $x$  axis. The energy properties are influenced by varying the parameter  $\omega/B$ . When

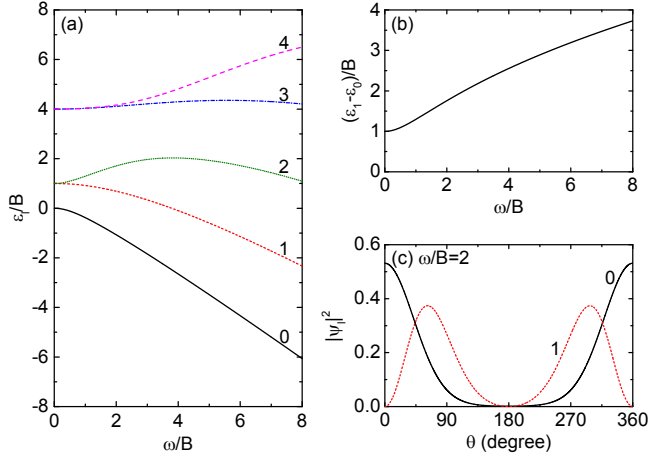


FIG. 2. (a) Energies  $\varepsilon_l/B$  as a function of the parameter  $\omega/B$ . The energy difference between the ground and first excited states is shown in (b). (c) Probability densities  $|\psi_l|^2$  of the ground and first excited states as a function of the angle  $\theta$  for  $\omega/B = 2$ . The tilt angle is  $\theta_t = 0^\circ$ .

the field is absent, all excited states are two-fold degenerate except for the ground state at  $\omega/B = 0$ . Due to the presence of dipole-field interaction, the degenerate levels are split off at  $\omega/B \neq 0$ . The energy structure differs from that of a three-dimensional rotor [29, 30]. For the lowest two states, the energies  $\varepsilon_0$  and  $\varepsilon_1$  display decreasing behavior with increasing the parameter  $\omega/B$ . The energy difference between the two levels is gradually increased from  $B$  [see Fig. 2(b)]. For instance, a difference of  $1.75B$  is determined at  $\omega/B = 2$ . Correspondingly, in Fig. 2(c) the probability densities of the two states are modulated to spread along the  $x$  axis. As a whole, the energies are the same at arbitrary  $\theta_t$ , whereas the spatial distributions of the wave functions depend on the field direction. It is worth noting that, as defined in Eq. (7), a two-level subsystem is built from the two individual states  $|\psi_0\rangle$  and  $|\psi_1\rangle$ . However, the two states  $|\psi_1\rangle$  and  $|\psi_2\rangle$  are degenerate at  $\omega/B = 0$ , and thus have the same energies  $\varepsilon_1 = \varepsilon_2 = B$  [17]. The corresponding wave function is either  $\exp(i\theta)/\sqrt{2\pi}$  or  $\exp(-i\theta)/\sqrt{2\pi}$ . At  $\omega/B = 0$ , the transition between the states  $|\psi_0\rangle$  and  $|\psi_2\rangle$  can occur as well as the transition between the states  $|\psi_0\rangle$  and  $|\psi_1\rangle$ . The two-level subsystem fails in this situation. As a result, to generate entanglement based on coupled two-level subsystems, the tuning of  $\omega/B = 0$  is excluded throughout the calculation.

In Eq. (8) the energy  $E_n$  and the state  $|\Psi_n\rangle$  depend on these factors. The properties of the wave function plays a determinant role in the contribution of the factors. In Figs. 3(a) and (b) an electric field of fixed strength is oriented to modulate the spatial distribution of the wave function so that the absolute values of the factors become angle-dependent. By increasing  $\theta_t$ , the value  $|C_X|$  inversely varies against  $|C_0|$  and  $|C_1|$ . The features of  $|S_\alpha|$  are similar to those of  $|C_\alpha|$ . If the tilt angle is  $\theta_t = 0^\circ$  or  $90^\circ$ , the values of the factors will be either real or purely

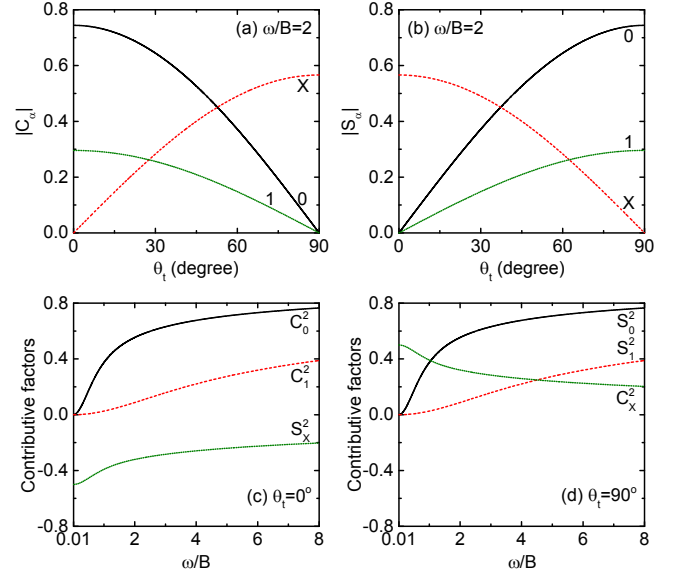


FIG. 3. Absolute values  $|C_\alpha|$  (a) and  $|S_\alpha|$  (b) of the factors as a function of the tilt angle  $\theta_t$  for  $\omega/B = 2$ . Square values  $C_\alpha^2$  (c) and  $S_\alpha^2$  (d) of the contributive factors as a function of the parameter  $\omega/B$  for  $\theta_t = 0^\circ$  and  $90^\circ$ .

imaginary. For  $\theta_t = 0^\circ$ , only  $|C_0|$ ,  $|C_1|$ , and  $|S_X|$  are contributive and maximal, whereas  $|S_0|$ ,  $|S_1|$ , and  $|C_X|$  are zero. A reverse situation occurs for  $\theta_t = 90^\circ$  where the contributive roles are interchanged to be  $|S_0|$ ,  $|S_1|$ , and  $|C_X|$ . To probe the two cases, the square values of the contributive factors are shown in Figs. 3(c) and (d). We simply set the initial value of  $\omega/B$  as 0.01 to avoid the three-level situation mentioned above. The relations  $C_0^2 = S_0^2$ ,  $C_1^2 = S_1^2$ , and  $C_X^2 = -S_X^2$  hold at arbitrary  $\omega/B$ . The magnitudes of  $C_0^2$  and  $C_1^2$ , as well as those of  $S_0^2$  and  $S_1^2$ , are raised by increasing the parameter  $\omega/B$ . On the contrary,  $C_X^2$  and  $S_X^2$  are close to zero at large  $\omega/B$ .

The entanglement property is analyzed in an electric field of a specific tilt angle. Figure 4(a) shows the four energy levels for  $\theta_t = 0^\circ$  and  $\Omega/B = 0.8$ . In this situation the field direction is parallel to the intermolecular direction. The energies are gradually diminished by increasing  $\omega/B$ . The corresponding concurrences reveal pronounced features as illustrated in Fig. 4(b). The concurrence for  $|\Psi_1\rangle$  is equal to that for  $|\Psi_4\rangle$ . Both values are decreased by increasing  $\omega/B$ . By contrast, the states  $|\Psi_2\rangle$  and  $|\Psi_3\rangle$  have the maximum concurrences  $C = 1$  all the time. When the electric field is applied perpendicular to the intermolecular direction, the decreasing energies in Fig. 4(c) are similar to those for  $\theta_t = 0^\circ$ . However, the energy structures are different in the two cases. For example, the difference between  $E_1$  and  $E_2$  for  $\theta_t = 0^\circ$  is greater than that for  $\theta_t = 90^\circ$ . Different from the case of  $\theta_t = 0^\circ$ , a local minimum for  $\theta_t = 90^\circ$  is observed at  $\omega/B \simeq 0.299$ , i.e., an anticrossing occurs [see insets of Fig. 4]. In Fig. 4(d) the overlapping features of concurrences also occur in the case of  $\theta_t = 90^\circ$ . The concu-

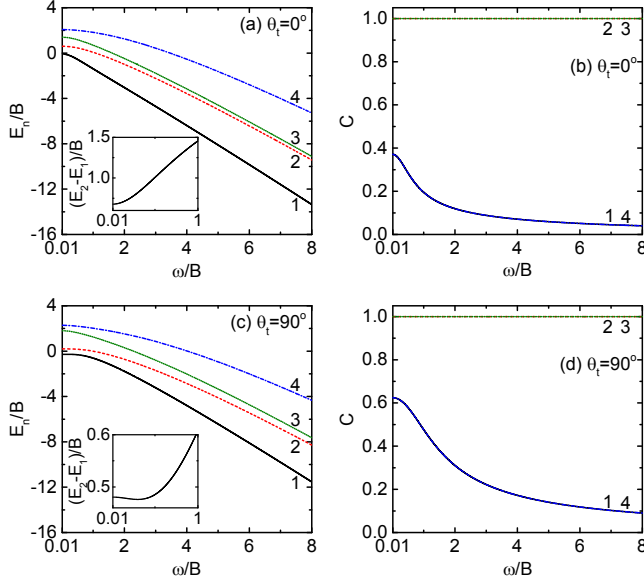


FIG. 4. Energies  $E_n/B$  (a) and concurrences  $C$  (b) as a function of the parameter  $\omega/B$  for  $\theta_t = 0^\circ$ . (c) and (d) correspond to  $\theta_t = 90^\circ$ . The insets show the difference between the energies  $E_1$  and  $E_2$ . The fixed parameter is  $\Omega/B = 0.8$ .

rences for  $|\Psi_2\rangle$  and  $|\Psi_3\rangle$  are still  $C = 1$ , while the same concurrences for  $|\Psi_1\rangle$  and  $|\Psi_4\rangle$  are higher than those in Fig. 4(b).

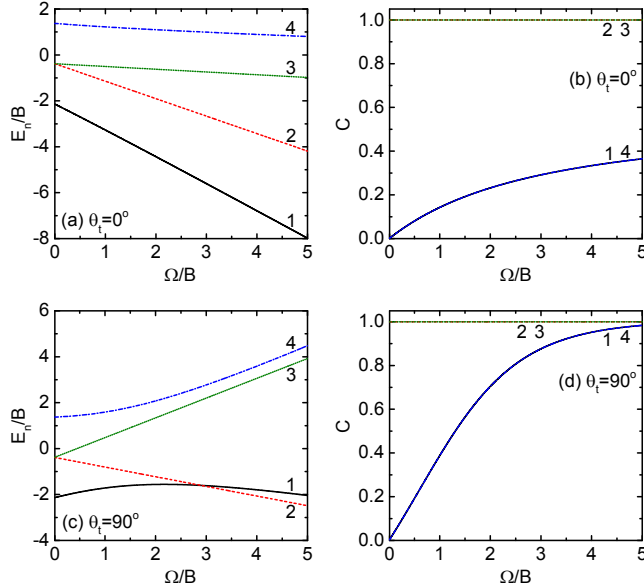


FIG. 5. Energies  $E_n/B$  (a) and concurrences  $C$  (b) as a function of the parameter  $\Omega/B$  for  $\theta_t = 0^\circ$ . (c) and (d) correspond to  $\theta_t = 90^\circ$ . The fixed parameter is  $\omega/B = 2$ .

Next, we turn to examining the effect of dipole-dipole interaction on the energies and concurrences by fixing the strength of the dipole-field interaction. The fixed parameter is set to be  $\omega/B = 2$ , corresponding to  $\varepsilon_0 = -1.07B$  and  $\varepsilon_1 = 0.68B$  in Fig. 2. By increasing the parameter

$\Omega/B$ , the four levels for  $\theta_t = 0^\circ$  reveal decreasing features [see Fig. 5(a)]. The energy differences between the adjacent levels increase at large  $\Omega/B$ . However, in Fig. 5(c) a diverse energy structure is obtained for  $\theta_t = 90^\circ$ . The levels for  $E_1$  and  $E_2$  have a crossing at  $\Omega/B \simeq 2.9$ . Increasing behavior is observed for  $E_3$  and  $E_4$ . As shown in Figs. 5(b) and (d), these concurrences can be classified into two types, which are similar to those in Fig. 4. Such a result indicates that the overlapping property is robust against the modulation of dipole-dipole interaction. For a system of three-dimensional rotors, similar concurrences can be observed only when the parameter is  $\omega/B = 0$  [13]. Furthermore, the stronger dipole-dipole interaction obviously enhances the concurrences for  $|\Psi_1\rangle$  and  $|\Psi_4\rangle$ . The degree of enhancement on the concurrence is higher in the case of  $\theta_t = 90^\circ$ .

To gain insight into the distinctive entanglement properties, the matrix in Eq. (8) can be simplified according to the results in Fig. 3:

$$\tilde{H} = \begin{pmatrix} 2\varepsilon_0 + a & 0 & 0 & d \\ 0 & \varepsilon_0 + \varepsilon_1 + b & f & 0 \\ 0 & f & \varepsilon_0 + \varepsilon_1 + b & 0 \\ d & 0 & 0 & 2\varepsilon_1 + c \end{pmatrix}, \quad (12)$$

where the parameters  $a = -2\Omega C_0^2$ ,  $b = -2\Omega C_0 C_1$ ,  $c = -2\Omega C_1^2$ ,  $d = \Omega S_X^2$ , and  $f = \Omega |S_X|^2$  are for  $\theta_t = 0^\circ$  while  $a = \Omega S_0^2$ ,  $b = \Omega S_0 S_1$ ,  $c = \Omega S_1^2$ ,  $d = -2\Omega C_X^2$ , and  $f = -2\Omega |C_X|^2$  are for  $\theta_t = 90^\circ$ . After calculating the matrix, one obtains the Bell-like states

$$|\Psi_1\rangle = \frac{\Delta + \sqrt{d^2 + \Delta^2}}{\sqrt{2N_+}} |00\rangle - \frac{d}{\sqrt{2N_+}} |11\rangle, \quad (13)$$

$$|\Psi_{2(3)}\rangle = \frac{1}{\sqrt{2}} |01\rangle - \frac{1}{\sqrt{2}} |10\rangle, \quad (14)$$

$$|\Psi_{3(2)}\rangle = \frac{1}{\sqrt{2}} |01\rangle + \frac{1}{\sqrt{2}} |10\rangle, \quad (15)$$

$$|\Psi_4\rangle = \frac{\Delta - \sqrt{d^2 + \Delta^2}}{\sqrt{2N_-}} |00\rangle - \frac{d}{\sqrt{2N_-}} |11\rangle, \quad (16)$$

and their energies

$$E_1 = \varepsilon_0 + \varepsilon_1 + (a + c)/2 - \sqrt{d^2 + \Delta^2}, \quad (17)$$

$$E_{2(3)} = \varepsilon_0 + \varepsilon_1 + b - f, \quad (18)$$

$$E_{3(2)} = \varepsilon_0 + \varepsilon_1 + b + f, \quad (19)$$

$$E_4 = \varepsilon_0 + \varepsilon_1 + (a + c)/2 + \sqrt{d^2 + \Delta^2}, \quad (20)$$

with  $\Delta = \varepsilon_1 - \varepsilon_0 + (c - a)/2$ ,  $N_+ = d^2 + \Delta^2 + \Delta\sqrt{d^2 + \Delta^2}$ , and  $N_- = d^2 + \Delta^2 - \Delta\sqrt{d^2 + \Delta^2}$ . For  $\theta_t = 0^\circ$ , the subscripts 2 are used in Eqs. (14) and (18), corresponding to 3 used in Eqs. (15) and (19). The subscripts interchange for  $\theta_t = 90^\circ$ . The concurrence is also derived from the definition

$$C = 2|d_2^n d_3^n - d_1^n d_4^n|, \quad (21)$$

for the state  $|\Psi_n\rangle$  [31]. The concurrences for  $|\Psi_2\rangle$  and  $|\Psi_3\rangle$  are straightforwardly  $C = 1$ . The states  $|\Psi_1\rangle$  and  $|\Psi_4\rangle$  have the same concurrence

$$C = \frac{1}{\sqrt{1 + \Delta^2/d^2}}, \quad (22)$$

with

$$\frac{\Delta^2}{d^2} = \left[ \frac{\varepsilon_1 - \varepsilon_0 - \Omega(C_1^2 - C_0^2)}{\Omega S_X^2} \right]^2, \quad (23)$$

for  $\theta_t = 0^\circ$  and

$$\frac{\Delta^2}{d^2} = \left[ \frac{\varepsilon_1 - \varepsilon_0 + \Omega(S_1^2 - S_0^2)/2}{2\Omega C_X^2} \right]^2, \quad (24)$$

for  $\theta_t = 90^\circ$ . The analytic results obtained agree exactly with the energies and concurrences in Figs. 4 and 5. Once the particular field directions are selected, the four Bell-like states can jointly occur as shown in Eqs. (13-16). This situation corresponds to two pairs of identical concurrences. More importantly, the modulation of the dipole-field and dipole-dipole interactions does not destroy the coexistent characteristic of Bell-like states.

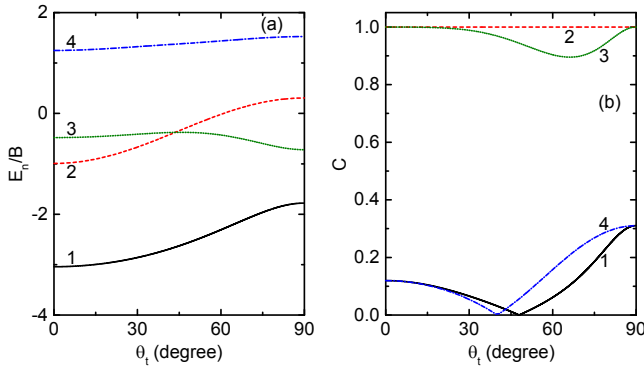


FIG. 6. Energies  $E_n/B$  (a) and concurrences  $C$  (b) as a function of the tilt angle  $\theta_t$  for  $\omega/B = 2$  and  $\Omega/B = 0.8$ .

When the tilt angle is not limited to  $\theta_t = 0^\circ$  and  $90^\circ$ , all factors become contributive to energy and concurrence. Figure 6(a) shows the angle-dependent energies for  $\omega/B = 2$  and  $\Omega/B = 0.8$ . Here the levels are labeled based on the case of  $\theta_t = 0^\circ$ ; this label is consistently retained throughout the tuning of  $\theta_t$ . The energies  $E_1$  and  $E_4$  vary monotonically with increasing  $\theta_t$ . By contrast, the energies  $E_2$  and  $E_3$  are modulated to intersect

at  $\theta_t \simeq 43.5^\circ$ . For  $\theta_t \neq 0^\circ$  and  $90^\circ$ , an explicit signature of entanglement is that the concurrences no longer coincide together [see Fig. 6(b)]. Only the state  $|\Psi_2\rangle$  retains the maximum concurrence  $C = 1$ , corresponding to  $(|01\rangle - |10\rangle)/\sqrt{2}$  throughout the modulation of  $\theta_t$ . The other states are composed of the four basis states in Eq. (7), whose concurrences are smaller than 1. The result implies that the four Bell-like states do not jointly exist at  $\theta_t \neq 0^\circ$  and  $90^\circ$ . Specifically, due to the angle-dependency of the factors, the concurrences for  $|\Psi_1\rangle$  and  $|\Psi_4\rangle$  are modulated to be greatly reduced at  $\theta_t \simeq 47.9^\circ$  and  $40^\circ$ , respectively.

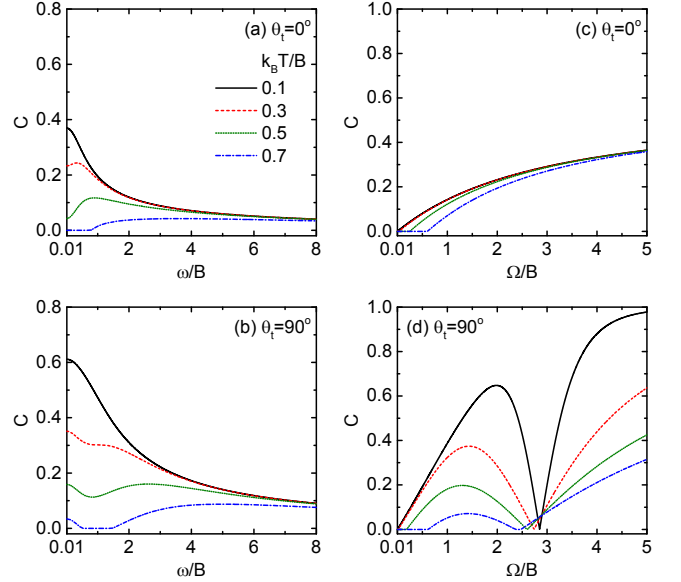


FIG. 7. Concurrences  $C$  for  $\theta_t = 0^\circ$  and  $90^\circ$  as a function of the parameters  $\omega/B$  and  $\Omega/B$  at different temperatures. (a) and (b) correspond to  $\Omega/B = 0.8$  while  $\omega/B = 2$  is used in (c) and (d).

The thermal influence on the entanglement is analyzed, specifically with respect to the Bell-like states. Figures 7(a) and (b) show the temperature-related concurrences by varying the parameter  $\omega/B$ . Since the temperature induces the contribution of the four Bell-like states, the mixing effect leads to a suppressed concurrence [see Eq. (9)]. When the temperature is raised, the degree of reduction of concurrence is enlarged. Although the concurrences for  $\theta_t = 0^\circ$  and  $90^\circ$  are similar, two dissimilar suppressed features occur, especially in the region of small  $\omega/B$ . This result originates from the two different energy structures, as illustrated in Figs. 4(a) and (c). Furthermore, the properties of the energy structure strongly affect the concurrences that are dependent on the parameter  $\Omega/B$  [see Figs. 7(c) and (d)]. Different from smooth features for  $\theta_t = 0^\circ$ , greatly suppressed concurrences can be obtained around the point where an energy crossing between  $E_1$  and  $E_2$  occurs for  $\theta_t = 90^\circ$ , as depicted in Figs. 5(a) and (c).

## IV. CONCLUSIONS

We have investigated the entanglement properties in a system of two-dimensional polar molecules by applying an electric field. The electric field parameters modulate the two-dimensional rotation, leading to distinctive energy spectra and concurrence. When the field direction is perpendicular or parallel to the intermolecular direction, the concurrences become overlapping. The four Bell-like states are collectively generated in the two situations. The coexistence of Bell-like states steadily holds against the modulation of the dipole-field and dipole-dipole in-

teractions. Once other field directions are selected, these significant properties will be destroyed. Instead, the concurrences can be greatly reduced in certain field directions. The concurrences for the Bell-like states are further analyzed at finite temperatures. The different energy structures cause diverse suppressed features in the two situations.

## ACKNOWLEDGMENTS

This work is supported by the Ministry of Science and Technology of Taiwan under Grant No. 103-2112-M-390-003-MY3.

- 
- [1] T. Wilk, S. C. Webster, A. Kuhn, and G. Rempe, *Science* **317**, 488 (2007).
  - [2] B. Weber, H. P. Specht, T. Müller, J. Bochmann, M. Mücke, D. L. Moehring, and G. Rempe, *Phys. Rev. Lett.* **102**, 030501 (2009).
  - [3] P. Neumann, N. Mizuochi, F. Rempp, P. Hemmer, H. Watanabe, S. Yamasaki, V. Jacques, T. Gaebel, F. Jelezko, and J. Wrachtrup, *Science* **320**, 1326 (2008).
  - [4] M. D. Shulman, O. E. Dial, S. P. Harvey, H. Bluhm, V. Umansky, and A. Yacoby, *Science* **336**, 202 (2012).
  - [5] L. Amico, R. Fazio, A. Osterloh, and V. Vedral, *Rev. Mod. Phys.* **80**, 517 (2008).
  - [6] R. Horodecki, P. Horodecki, M. Horodecki, and K. Horodecki, *Rev. Mod. Phys.* **81**, 865 (2009).
  - [7] C. H. Bennett and S. J. Wiesner, *Phys. Rev. Lett.* **69**, 2881 (1992).
  - [8] C. H. Bennett, G. Brassard, C. Crépeau, R. Jozsa, A. Peres, and W. K. Wootters, *Phys. Rev. Lett.* **70**, 1895 (1993).
  - [9] M. Żukowski, A. Zeilinger, M. A. Horne, and A. K. Ekert, *Phys. Rev. Lett.* **71**, 4287 (1993).
  - [10] D. DeMille, *Phys. Rev. Lett.* **88**, 067901 (2002).
  - [11] M. Karra, K. Sharma, B. Friedrich, S. Kais, and D. Herschbach, *J. Chem. Phys.* **144**, 094301 (2016).
  - [12] J. X. Han, Y. Hu, Y. Jin, and G. F. Zhang, *J. Chem. Phys.* **144**, 134308 (2016).
  - [13] Q. Wei, S. Kais, B. Friedrich, and D. Herschbach, *J. Chem. Phys.* **134**, 124107 (2011).
  - [14] Q. Wei, S. Kais, B. Friedrich, and D. Herschbach, *J. Chem. Phys.* **135**, 154102 (2011).
  - [15] E. Charron, P. Milman, A. Keller, and O. Atabek, *Phys. Rev. A* **75**, 033414 (2007).
  - [16] K. Mishima and K. Yamashita, *J. Chem. Phys.* **130**, 034108 (2009).
  - [17] D. H. McIntyre, *Quantum Mechanics: A Paradigms Approach* (Pearson Addison-Wesley, San Francisco, 2012).
  - [18] K. Svensson, L. Bengtsson, J. Bellman, M. Hassel, M. Persson, and S. Andersson, *Phys. Rev. Lett.* **83**, 124 (1999).
  - [19] L. Bengtsson, K. Svensson, M. Hassel, J. Bellman, M. Persson, and S. Andersson, *Phys. Rev. B* **61**, 16921 (2000).
  - [20] D. Teillet-Billy and J. P. Gauyacq, *Surf. Sci.* **502-503**, 358 (2002).
  - [21] U. Landman, G. G. Kleiman, C. L. Cleveland, E. Kuster, R. N. Barnett, and J. W. Gadzuk, *Phys. Rev. B* **29**, 4313 (1984).
  - [22] Y. T. Shih, Y. Y. Liao, and D. S. Chuu, *Phys. Rev. B* **68**, 075402 (2003).
  - [23] H. Shima and T. Nakayama, *Phys. Rev. A* **70**, 013401 (2004).
  - [24] H. Shima and T. Nakayama, *Phys. Rev. B* **71**, 155210 (2005).
  - [25] T. Iwata and M. Watanabe, *Phys. Rev. B* **81**, 014105 (2010).
  - [26] W. K. Wootters, *Phys. Rev. Lett.* **80**, 2245 (1998).
  - [27] M. C. Arnesen, S. Bose, and V. Vedral, *Phys. Rev. Lett.* **87**, 017901 (2001).
  - [28] X. Wang, *Phys. Lett. A* **281**, 101 (2001).
  - [29] K. von Meyenn, *Z. Phys.* **231**, 154 (1970).
  - [30] J. M. Rost, J. C. Griffin, B. Friedrich, and D. R. Herschbach, *Phys. Rev. Lett.* **68**, 1299 (1992).
  - [31] T. Yu and J. H. Eberly, *Phys. Rev. B* **66**, 193306 (2002).